AD_____

Award Number: DAMD17-01-1-0243

TITLE: Alterations in Gene Transcription by Physiological Stress: A Mechanism for Drug Resistance Through NF-κB Activation

PRINCIPAL INVESTIGATOR: Lori M. Brandes

CONTRACTING ORGANIZATION: The George Washington University
Washington, DC 20052

REPORT DATE: June 2002

TYPE OF REPORT: Annual Summary

PREPARED FOR: U.S. Army Medical Research and Materiel Command
Fort Detrick, Maryland 21702-5012

REPORT DOCUMENTATION PAGE

Form Approved
OMB No. 074-0188

1. AGENCY USE ONLY (Leave blank)	2. REPORT DATE	3. REPORT TYPE AND DATES COVERED
	June 2002	Annual Summary (1 June 2001 - 31 May 2002)

4. TITLE AND SUBTITLE
Alterations in Gene Transcription by Physiological Stress: A Mechanism for Drug Resistance Through NF-kB Activation

5. FUNDING NUNUMBER
DAMD17-01-1-0243

6. AUTHOR(S)
Lori M. Brandes

7. PERFORMING ORGANIZATION NAME(S) AND ADDRESS(ES)
The George Washington University
Washington, DC 20052

email - phmlmb@gwumc.edu

8. PERFORMING ORGANIZATION REPORT NUMBER

9. SPONSORING / MONITORING AGENCY NAME(S) AND ADDRESS(ES)
U.S. Army Medical Research and Materiel Command
Fort Detrick, Maryland 21702-5012

10. SPONSORING / MONITORING AGENCY REPORT NUMBER

11. SUPPLEMENTARY NOTES
Report contains color

12a. DISTRIBUTION / AVAILABILITY STATEMENT
Approved for Public Release; Distribution Unlimited

12b. DISTRIBUTION CODE

13. ABSTRACT *(Maximum 200 Words)*

One of the major limiting factors to the successful treatment of breast cancer is the development of drug resistance. Adverse conditions associated with solid tumor progression, which trigger cellular stress responses, may underlie the mechanisms of intrinsic chemotherapeutic drug resistance. EMT6 mouse mammary tumor cells treated with the chemical stress agent, brefeldin A (BFA) or the physiologic stress, hypoxia develop comparable levels of resistance to the topoisomerase II inhibitor, etoposide. To determine common mechanisms for chemical- and physiologic-induced drug resistance, we have performed expression analysis of stress-treated EMT6 cells. BFA or hypoxia treatment result in enhanced expression of transforming growth factor-β (TGF-β) and decreased expression of the platelet-derived growth factor receptor, PDGFRα, and the mitogen-activated protein kinase (MAPK), MEK1. Western blot analysis confirms increased TGF-β protein and reduced PDGFRα and phospho-MEK1/2 levels with stress treatment. In vitro studies show treatment with TGF-β, anti-PDGFRα blocking antibodies, or inhibition of MEK1/2 with U0126 treatment are sufficient to cause etoposide resistance. These results provide evidence for TGF-β activation and down-regulation of the PDGFRα/MAPK signaling pathway in the development of tumor drug resistance and suggest that modulation of TGF-β, PDGFRα or the MAPK cascade may enhance the clinical effectiveness of conventional anticancer chemotherapies.

14. SUBJECT TERMS	15. NUMBER OF PAGES
breast cancer, drug resistance, stress, NF-κB, gene array, hypoxia	42
	16. PRICE CODE

17. SECURITY CLASSIFICATION OF REPORT	18. SECURITY CLASSIFICATION OF THIS PAGE	19. SECURITY CLASSIFICATION OF ABSTRACT	20. LIMITATION OF ABSTRACT
Unclassified	Unclassified	Unclassified	Unlimited

Table of Contents

Introduction

The objective of this research has been to understand the mechanisms by which physiologic-based drug resistance develops in cancer cells. Physiologic stressors, such as hypoxia, induce cellular stress responses and survival in the presence of anticancer agents. We have shown EMT6 mouse mammary tumor cells treated with hypoxia or the chemical stress agent brefeldin A develop resistance to topoisomerase II inhibitors and that BFA- and hypoxia-induced resistance to etoposide is mediated by the transcription factor NF-κB in the EOR stress pathway. It has been long understood that topoisomerase II inhibitors exert their cytotoxicity through the induction of apoptosis in cancer cells. In addition, NF-κB itself is known to mediate the expression many known antiapoptotic genes. Taken together, these data suggest that stress-induced NF-κB activation may result in resistance to topoisomerase II inhibitors through enhanced expression of NF-κB-dependent genes, including antiapoptotic genes. We therefore hypothesized that stress-induced drug resistance through NF-κB activation results in upregulation of a select group of NF-κB-regulated genes.

Body

We have shown that treatment of EMT6 mouse mammary tumor cells with the chemical stress, BFA or the physiologic stress, hypoxia results in resistance to topoII inhibitors (1-3). To determine if a common mechanism underlies the development of BFA- and hypoxia-induced drug resistance, we performed expression analysis of stress-treated EMT6 cells. In preparation for experiments with PON induction of IκBαM cells, we examined stress responses of vector-transfected cells treated with PON. VCT cells were treated with 10 μg/ml BFA for 2 h, followed by a BFA-free recovery for 6 h, or with hypoxia for 8 h. Total RNA was collected from stress-treated cells, converted into double-stranded biotin-labeled RNA, and hybridized onto Mu11K GeneChips as detailed in Materials and Methods. The fluorescence intensity of RNA probe bound to the GeneChip was measured and converted to a quantitative relative fluorescence intensity using the Affymetrix software. Data sets were compared using the Affymetrix software after correcting for variations in background fluorescence intensity and variations in probe binding affinity between profiles to determine the fold-change in expression between two data sets. Each RNA probe constructed was hybridized to a different GeneChip twice to generate two expression profiles for each treatment. Each duplicate set of data was compared to another duplicate set by a 4-way pair-wise comparison, generating four comparison data sets which were combined to generate a mean change in expression for a given comparison.

Figure 1 shows the specific expression profiles that were determined (Appendices, Figure 1, boxes) and the comparisons of those data sets that were performed (Figure 1, arrows). For each comparison, lists of genes with 2-fold and greater changes and 5-fold and greater changes were generated. Candidate genes involved in the BFA-induced stress response (Figure 1, arrow 1) were determined by comparing the expression profiles of BFA-treated VCT cells induced with PON (Figure 1, VCT+PON+BFA) relative to non-stressed VCT cells induced with PON (Figure 1, VCT+PON). Likewise, candidate genes involved in the HYX-induced stress response (Figure 1, arrow 2) were determined by comparing the expression profiles of HYX-treated VCT cells induced with PON (Figure 1, VCT+PON+HYX) relative to non-stressed VCT cells induced with PON (Figure 1, VCT+PON). Next, the intersection of the BFA stress response and HYX stress response lists was used to identify those genes commonly up- or down-regulated in both BFA and HYX stress responses (Figure 1, arrow 3).

The global changes in gene expression with BFA or HYX treatment are shown in Figure 2. BFA stress caused the up-regulation of 1469 genes and the down-regulation of 1212 genes at levels greater than or equal to 2-fold (Figure 2, #1). Of the 491 total genes altered at 5-fold and greater levels with BFA stress, 263 were up-regulated and 228 were down-regulated (Figure 2, #1). HYX stress resulted in the up-regulation of 1902 genes and the down-regulation of 1707 genes at 2-fold and greater levels and the up-regulation of 187 genes and the down-regulation of 168 genes at 5-fold and greater levels (Figure 2, #2). Intersection of the BFA and HYX profiles resulted in 8 genes up-regulated and 4 genes down-regulated in both stress profiles when using looking at genes altered 5-fold and greater and 39 genes up-regulated and 31 genes down-regulated in both profiles when looking at genes altered 2-fold and greater (Figure 2, #3).

Our rapidly growing knowledge of genome sequence and the large data sets generated in microarray experiments have made analysis of such experiments beyond the capacities of an individual's knowledge base. The use of bioinformatics tools to aid in the analysis of array data is now an essential part in understanding microarray results. In this study, two gene expression bioinformatics databases were used to determine the general functional classification of the genes involved in either the BFA, the HYX or both BFA and HYX stress responses. The DRAGON database (Database Referencing of Array Genes ONline, www.kennedykrieger.org/pevsnerlab/dragon.htm), developed by the Pevsner laboratory of the Kennedy Krieger Institute, consists of information derived from several publicly available databases, including UniGene, SWISS-PROT and OMIM. The HAPI database (High-density Array Pattern Interpreter, www.array.ucsd.edu/hapi/) provides a similar integrated overlook, plus other advanced statistical programs for hierarchical clustering and Self-Organizing Maps. After the mean fold change in expression with stress treatment was calculated, we uploaded the Genbank identification number for each gene altered at 2-fold and greater levels into the DRAGON and HAPI databases to determine the general functional categories for the genes involved in BFA, HYX and both BFA and HYX stress responses. Figure 3 shows the predominant functional categories of genes altered with BFA stress are cell signaling, transcription, and cell adhesion. There were also significant percentages of genes involved in tumor growth and stress responses (Figure 3). HYX stress resulted in a similar distribution, however a relatively larger percentage of genes were found to be associated with apoptosis (Figure 3). Genes involved in both the BFA and HYX-induced stress responses were primarily involved in cell signaling, transcription, tumor growth, apoptosis and protein modification (Figure 3).

Figure 4 shows the identities of the genes similarly up- or down-regulated at 2-fold and greater levels during BFA and hypoxic stress treatment. Of particular interest were the changes observed in the transforming growth factor-beta (TGF-β), the platelet-derived growth factor receptor-alpha (PDGFRα) and the MEK1 protein kinase (Figure 4). TGF-β has a well-defined role in tumorigenesis, tumor progression and tumor drug resistance (4-5). TGF-β is also known to control expression of PDGFRα, which is also associated with tumor growth and the development of drug resistance (6-7). Studies have shown PDGFRα often signals through the mitogen activated protein kinases, of which MEK1 is a member (8-9). Since both PDGFRα and MEK1 were down-regulated with stress, this suggests downregulation of the PDGFRα/MAPK pathway may be involved in the development of stress-induced drug resistance. Given the role of TGF-β in drug resistance, NF-κB activation and in PDGFRα expression, we also explored the involvement of TGF-β in stress-induced drug resistance.

After identifying genes for further evaluation, we determined if the changes in TGF-β, PDGFRα and MEK1 expression were also detectable on the protein level. For protein validation, whole cell lysates from EMT6 cells treated with 10 μg/ml BFA for 2 h, followed by a BFA-free recovery for 6 h or HYX for 8 h were collected and analyzed by western blot. The relative band intensities of each protein from four independent experiments were quantitated and the mean fold change in protein levels compared to non-stressed control were determined (Figure 5). Figure 5 shows that TGF-β protein levels are significantly elevated and PDGFRα protein levels are reduced with either BFA or HYX treatment, as was suggested in the expression data (Figure 5). MEK1 total

protein levels did not change with BFA or hypoxic stress, however analysis with an antibody selective for phosphorylated forms of MEK1 and MEK2 (phospho-MEK1/2) protein shows that stress does cause decreased MEK1/2 phosphorylation (Figure 5). MEK2 total protein levels were constant during either BFA or HYX stress (Figure 5). As a control, protein from EMT6 cells treated with the stress agent castanospermine (CAS) was also collected. We have previously shown that CAS treatment does not activate NF-κB or the EOR stress response and does not cause resistance to the topoII inhibitor teniposide (1). Figure 5 shows treatment with 10 μg/ml CAS for 6 h does not cause significant alterations in TGF-β, PDGFRα, MEK1, MEK2, or phosphorylated MEK1/2.

Our data show that TGF-β mRNA and protein levels are enhanced with BFA or HYX stress (Figures 4 and 5). To determine if TGF-β treatment is sufficient to cause drug resistance, EMT6 cells were treated with 0.1 or 1.0 ng/ml TGF-β for 8 h (a duration equivalent to BFA and HYX treatments). During the last hour of TGF-β treatment, 25 or 50 μM etoposide was added prior to analysis of cell survival by colony forming assay. Our data show that TGF-β treatment reduces sensitivity to etoposide compared to non-treated control cells (Figure 6).

TGF-β is known to modulate levels of PDGFRα, which in turn mediates phosphorylation of the MAPK members MEK and ERK (Jennings et al., 1997; Conway et al., 1999). Given that we observed reduced PDGFRα and phospho-MEK1/2 levels with stress treatment (Figure 5), we determined the effects of TGF-β treatment on PDGFRα and MEK protein levels (Figure 7). EMT6 cells were treated with 0.1 or 1.0 ng/ml TGF-β for 8 h. Whole cell lysates from TGF-β-treated cells or untreated control cells were collected and analyzed by western blot using anti- PDGFRα, anti-MEK1, anti-MEK2, and anti-phospho-MEK1/2 primary antibodies. Figure 7 shows TGF-β treatment does not change total MEK1 or MEK2 protein, but does result in a significant decrease in PDGFRα and phospho-MEK1/2 protein levels.

The platelet-derived growth factor receptor PDGFRα has been associated with tumor growth and tumor drug resistance (7) and has been associated with induction of the MAPK signaling pathway (9). The data presented here show that PDGFRα and phospho-MEK1/2 protein levels are reduced (Figure 4) by stress conditions known to cause resistance to topoII inhibitors (1-3). To determine if inhibition of PDGFRα results in the development of resistance to etoposide, EMT6 cells were treated with 1 or 10 ng/ml anti-PDGFRα antibody for 8 h (a duration equivalent to BFA and hypoxia treatments). The concentration of blocking antibody used was chosen based upon the ND_{50} value provided in the manufacturer's product information insert (R&D Systems). During the last hour of treatment, 25 or 50 μM etoposide was added prior to colony forming assay. Our data show that inhibition of PDGFRα with blocking antibodies results in the development of relatively small, but significant levels of resistance to 50 μM etoposide (Figure 8). Western blot analysis of lysates from EMT6 cells treated with 1.0 and 10 ng/ml anti-PDGFRα blocking antibody show reduced phosphorylated MEK1/2 protein levels and no change in MEK1 or MEK2 protein levels (Figure 9).

Our data show that chemical and physiologic stress treatments known to cause resistance to etoposide (1-3) reduce levels of phosphorylated MEK1/2 protein (Figure 5). To determine if direct inhibition of MEK phosphorylation is sufficient to cause drug resistance, we tested the effects of U0126, a selective inhibitor of MEK1/2

phosphorylation, on etoposide toxicity. EMT6 cells were treated with 10 or 30 μM U0126 for a total of 8 h (a duration equivalent to that of BFA and HYX). During the last hour of U0126 treatment, cells were exposed to 25 or 50 μM etoposide for one hour prior to analysis by colony forming assay. Figure 10 shows that U0126 treatment results in the development of resistance to etoposide. PDGFRα is also capable of activating other members of the MAPK family, including the stress-activated protein kinases (SAPK) (9). To test whether other MAPK pathways may be involved in the development of etoposide resistance, we treated EMT6 cells with the selective p38 SAPK inhibitor SB203580. Treatment with 10 μM SB203580 did not result in significant alteration of etoposide toxicity (Figure 10). U0126
treatment did not change in MEK1 or MEK2 total protein levels in lysates from EMT6 cells analyzed by western blot, but significantly reduced phosphorylated MEK1/2 protein levels (Figure 11). SB203580 did not change MEK1, MEK2 or phosphorylated MEK1/2 levels (Figure 11).

We have shown expression of IκBαM prevents chemical and physiologic stress-induced resistance to etoposide (3). To determine if a common mechanism underlies the reversal of BFA- and HYX-induced drug resistance with IκBαM expression, we performed expression analysis of stress-treated cells using oligonucleotide GeneChip arrays (Affymetrix). Figure 1 shows the specific expression profiles collected (Figure 1, boxes) and the comparisons of those data sets performed. For each comparison, mean fold-changes of greater than or equal to 2-fold and greater than for equal to 5-fold and greater were generated. Candidate genes involved in reversal of BFA-induced drug resistance (Figure 1, #4) were determined by comparing the expression profiles of BFA-treated VCT cells induced with PON (VCT+PON+BFA, Figure 1) relative to BFA-treated IκBαM cells induced with PON (IκBαM+PON+BFA, Figure 1). Likewise, candidate genes involved in the reversal of HYX-induced drug resistance (Figure 1, #5) were determined by comparing the expression profiles of HYX-treated VCT cells induced with PON (VCT+PON+HYX, Figure 1) relative to HYX-treated IκBαM cells induced with PON (IκBαM+PON+HYX, Figure 1). To identify genes common to the reversal of both BFA- and HYX-induced drug resistance with IκBαM expression, we took the intersection of the genes involved in reversal of BFA-induced resistance and the genes involved in reversal of HYX-induced resistance (Figure 1, #6).

The global changes in gene expression during the reversal of BFA- or HYX-induced drug resistance with IκBαM expression are shown in Figure 12. Analysis of the expression profiles from BFA-treated IκBαM cells with respect to the expression profiles from BFA-treated VCT cells revealed 2149 genes up-regulated and 1329 genes down-regulated at 2-fold and greater levels and 25 genes up-regulated and 17 genes down-regulated at 5-fold and greater levels (Figure 12, #4). 873 genes were up-regulated and

574 genes were down-regulated at 2-fold and greater levels and 8 genes were up-regulated and 10 genes were down-regulated at 5-fold and greater levels during conditions of the reversal of HYX-induced drug resistance (Figure 12, #5). Intersection of these data resulted in 22 genes up-regulated and 18 genes down-regulated in the reversal of both BFA- and HYX-induced drug resistance when using looking at genes altered 2-fold and greater and no genes commonly regulated at 5-fold and greater levels (Figure 12, #6).

We uploaded the GenBank identification number for each gene altered at 2-fold and greater into the DRAGON and HAPI databases to determine the general functional categories for the genes involved in the reversal of BFA-, HYX- and both BFA- and HYX-induced resistance with IκBαM expression. Figure 13A shows the predominant functional categories of genes altered during the reversal of BFA-induced resistance are tumor growth, apoptosis, cell signaling, transcription, and cell adhesion. HYX stress resulted in a relatively larger percentage of genes involved in tumor growth, apoptosis and cell cycle (Figure 13B). Genes involved in both the BFA and HYX-induced stress responses were far less likely to be involved in tumor growth and apoptosis and were primarily involved in cell adhesion, signaling, and transcription (Figure 13C). Figure 14 lists the genes identified as similarly up- or down-regulated at 5-fold and greater levels when comparing the profiles of BFA-treated IκBαM cells relative to BFA-treated VCT cells (#4 comparison from Figure 12). The candidate genes altered 5-fold and greater in the reversal of HYX-induced drug resistance with IκBαM are shown in Figure 15 (#5 comparison from Figure 12). The genes commonly altered at 2-fold and greater levels during the reversal of BFA- and HYX-induced resistance are shown in Figure 16 (#6 comparison from Figure 12).

After analysis with the HAPI and DRAGON databases, the 40 candidate genes involved in the reversal of BFA- and HYX-induced resistance did not reveal any of the more common signaling pathway proteins that would provide insight into the mechanism of reversal of stress-induced resistance with IκBαM expression. In the data presented here, RNA was collected from stress-treated cells for expression analysis after 8 h of stress to correspond with the time point colony forming experiments occurred. However, our previous time course data have shown that maximal NF-κB activation by hypoxic stress occurs after 2 h of treatment (1-3). Our preliminary data suggest that further study of the expression profiles of VCT and IκBαM cells treated with variable stress durations may reveal other candidate genes in the reversal of stress-induced drug resistance or in the BFA- and hypoxia-induced stress responses.

We then examined the role of NF-κB activation in the TGF-β/PDGFRα/MAPK pathway involved in the development of stress-induced drug resistance. Comparison of stress profiles from IκBαM cells to stress profiles from VCT cells revealed no significant changes in TGF-β, PDGFRα or MEK1 gene expression levels (Figure 16). These data suggested that stress-induced enhancement of TGF-β expression and inhibition of PDGFRα and MEK1 expression (observed in the comparisons of non-stressed to stress-treated VCT cells, Figure 4) was not dependent upon NF-κB activation. To test whether stress-induced alterations of TGF-β, PDGFRα, and MEK1 was dependent upon NF-κB activation, we analyzed protein expression of VCT and IκBαM cells treated with stress. VCT and IκBαM cells were induced with 10 μM ponasterone A (PON) for 24 h. Cells

were stress-treated in the presence of PON with 10 μg/ml brefeldin A (BFA) for 2 h followed by a 6 h BFA-free recovery or with hypoxia for 8 h. Protein lysates were collected and analyzed by western blot for expression of TGF-β and PDGFRα/MAPK proteins. Our data show that VCT and non-induced IκBαM cells have enhanced expression of TGF-β (Figure 18) and significantly reduced levels of PDGFRα (Figure 19) and phosphorylated-MEK1/2 (Figure 20) in the presence of stress. These findings agree with our data from non-transfected EMT6 cells treated with stress (Figure 5). However, stress treatment of IκBαM cells induced with PON did not cause significant alteration of TGF-β, PDGFRα or phosphorylated-MEK1/2. Taken together, these data suggest that the stress-induced alterations in TGF-β, PDGFRα and MEK phosphorylation are dependent upon NF-κB activation. These findings imply a mechanism for the development of drug resistance downstream of NF-κB activation involving up-regulation of TGF-β and down-regulation of the PDGFRα/MAPK signaling pathway. They further suggest a mechanism for the prevention of stress-induced drug resistance with IκBαM expression, whereby inhibition of NF-κB activation prevents the stress-induced alterations of TGF-β, PDGFRα and phosphorylated MEK. These data suggest that small molecules which alter NF-κB or the downstream TGF-β/PDGFRα/MEK pathway may enhance the therapeutic efficacy of conventional clinical cancer therapies by inhibiting the pathways that mediate stress-induced drug resistance.

Key Research Accomplishments

1. Identification of genes altered during BFA and hypoxia stress and during both stress responses and its general functional classification.

2. Protein and *in vitro* validation of select candidate genes (TGF-β, PDGFRα and MEK1) involved in stress-induced resistance.

3. Identification of genes altered in BFA and hypoxia stress responses with IκBαM expression.

4. Protein validation of the stress-induced TGF-β, PDGFRα and MEK with IκBαM expression.

Reportable Outcomes

Manuscripts

Brandes LM, Lin ZP, Patierno SR, Kennedy KA (2001) Reversal of physiological stress-induced resistance to topoisomerase II inhibitors using an inducible phosphorylation site-deficient mutant of IκBα. Mol Pharm. 60: 559-567.

Boller YC, Brandes LM, Russell RL, Lin ZP, Patierno SR, Kennedy KA (2001) Prostaglandin A1 inhibits stress-induced NF-κB activation and reverses resistance to topoisomerase II inhibitors. Oncol Res. 12: 383-395.

Brandes LM, Patierno SR, Kennedy KA. NF-κB activation mediates stress-induced resistance to topoisomerase II inhibitors and attenuates cellular responses to stress. Manuscript in preparation.

Brandes LM, Stephan DA, Peterson K, MacDonald T, Patierno SR, Kennedy KA. Expression analysis reveals a role for TGF-β and the PDGFRα/MAPK pathway in the development of etoposide drug resistance. Manuscript in preparation.

Abstracts Presented at Scientific Meetings

Brandes LM, Patierno SR, Stephan DA, Kennedy KA. Stress-induced resistance of breast tumor cells to topoisomerase II inhibitors is mediated by NF-κB activation. Soc Exper Biol Med. July 2001.

Brandes LM, Peterson K, Stephan DA, Kennedy KA. Expression profiling of chemical and physiologic stress-treated breast tumor cells reveals a signaling pathway for drug resistance through NF-κB activation. Amer Soc Cell Bio Abst. Dec 2001.

Brandes LM, Hadjisavva IS, Peterson K, Patierno SR, Stephan DA, Kennedy KA. Expression analysis reveals a role for TGF-β and the PDGFRα/MAPK signaling pathway in the development of both chemical- and physiologic-induced drug resistance of breast cancer cells. Amer Assoc Cancer Res Abst. April 2002.

Hadjisavva IS, Brandes LM, Stephan DA, Kennedy KA. Investigation of pathways involved with the development of stress-induced resistance of MDA-MB231 human cancer cells to topoisomerase II inhibitors. 7th Annual George Washington Health Sciences Research Day. April 2002.

Degrees Obtained/Supported by Award

Ph.D. in Pharmacology, May 2002, Lori Brandes, Principal Investigator

Conclusions

Expression profiling of stress-treated tumor cells revealed several genes commonly altered during BFA and hypoxia stress treatment. Western blot analysis of these data confirmed that BFA or hypoxia treatment result in enhanced TGF-β expression and diminished PDGFRα expression and MEK phosphorylation. *In vitro* studies showed TGF-β treatment causes etoposide resistance and reduces PDGFRα expression and MEK phosphorylation. Inhibition of PDGFRα also results in etoposide resistance and inhibition of MEK phosphorylation. Direct inhibition of MEK with U0126 decreased MEK phosphorylation concurrent with the development of resistance to etoposide. Taken together, these data suggest a putative mechanism for the development of both chemical and physiological stress-induced drug resistance through NF-κB activation whereby elevated TGF-β results in inhibition of the PDGFRα/MAPK signaling cascade. Our data further show that stress-treated IκBαM cells, which do not develop drug resistance, do not exhibit changes in TGF-β, PDGFRα or MEK. This suggests that NF-κB activation mediates stress-induced alterations in TGF-β and the PDGFRα/MAPK signaling and that inhibition of these downstream events may explain the prevention of stress-induced resistance with IκBαM expression. Furthermore, these data imply that alteration of NF-κB, TGF-β or the PDGFRα/MAPK cascade may also prove therapeutically useful in the treatment of solid tumors by preventing the development of stress responses that impact drug sensitivity.

References

1. Lin, Z. P., Boller, Y. C., Amer, S. M., Russell, R. L., Pacelli, K. A., Patierno, S. R. and Kennedy, K. A. (1998) Prevention of brefeldin A-induced resistance to teniposide by the proteasome inhibitor MG-132: involvement of NF-κB activation in drug resistance. Cancer Res. 58: 3059-3065.

2. Boller, Y. C., Brandes, L. M., Russell, R. L., Lin, Z. P., Patierno, S. R. and Kennedy, K. A. (2001) Prostaglandin A_1 inhibits stress-induced NF-κB activation and reverses resistance to topoisomerase II inhibitors. Oncology Res. 12: 383-395.

3. Brandes, L. M., Lin, Z. P., Patierno, S. R. and Kennedy, K. A. (2001) Reversal of physiological stress-induced resistance to topoisomerase II inhibitors using an inducible phosphorylation site-deficient mutant of IκBα. Mol Pharmacol. 60: 559-567.

4. de Winter, J. P., Roelen, B. A., ten Dijke, P., van der Burg, B. and van den Eijnden-van Raaij, A. J. (1997) DPC4 (SMAD4) mediates transforming growth factor-beta1 (TGF-beta1) induced growth inhibition and transcriptional response in breast tumor cells. Oncogene. 14: 1891-1899.

5. Arteaga, C. L., Koli, K. M., Dugger, T. C. and Clarke, R. (1999) Reversal of tamoxifen resistance of human breast carcinomas in vivo by neutralizing antibodies to transforming growth factor-beta. J Natl Cancer Inst. 91: 46-53.

6. Yoshida, K., Kuniyasu, H., Yasui, W., Kitadai, Y., Toge, T. and Tahara, E. (1993) Expression of growth factors and their receptors in human esophageal carcinomas: regulation of expression by epidermal growth factor and transforming growth factor alpha. J Cancer Res Clin Oncol. 119: 401-407.

7. Jennings, M. T., Hart, C. E., Commers, P. A., Witlock, J. A., Martincic, D., Macinuas, R. J., Moots, P. L. and Shehab, T. M. (1997) Transforming growth factor beta as a potential tumor progression factor among hyperdiploid glioblastoma cultures: evidence for the role of platelet-derived growth factor. J Neurooncol. 31: 233-254.

8. Choudhury, G. G., Karamitsos, C., Hernandez, J., Gentilini, A., Bardgette, J. and Abboud, H. E. (1997) PI-3-kinase and MAPK regulate mesangial cell proliferation and migration in response to PDGF. Am J Physiol. 273: 931-938.

9. Conway, A. M., Rakhit, S., Pyne, S. and Pyne, N. J. (1999) Platelet-derived-growth-factor stimulation of the p42/p44 mitogen-activated protein kinase pathway in airway smooth muscle: role of pertussis-toxin-sensitive G-proteins, c-Src tyrosine kinases and phosphoinositide 3-kinase. Biochem J. 337: 171-177.

Figure 1. Overview of Expression Analysis Comparisons

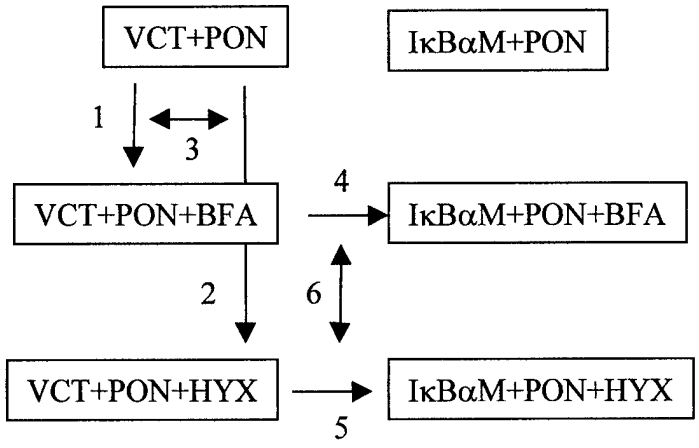

1. Changes in expression with BFA treatment in VCT cells treated with PON, *candidate genes involved in BFA-induced drug resistance*

2. Changes in expression with HYX treatment in VCT cells treated with PON, *candidate genes involved in HYX-induced drug resistance*

3. Genes commonly altered with either BFA or HYX stress in VCT cells treated with PON, *candidate genes involved in both BFA- and HYX-induced drug resistance*

4. Changes in expression of IκBαM+PON+BFA relative to VCT+BFA+PON, *candidate genes involved in the reversal of BFA-induced resistance with IκBαM*

5. Changes in expression of IκBαM+PON+HYX relative to VCT+HYX+PON, *candidate genes involved in the reversal of HYX-induced resistance with IκBαM*

6. Genes commonly altered in the comparisones of IκBαM+PON+BFA relative to VCT+BFA+PON and IκBαM+PON+HYX relative to VCT+HYX+PON, *candidate genes involved in the reversal of BFA- and HYX-induced resistance with IκBαM*

Comparisons	≥2-fold	+/-	≥5-fold	+/-
1. VCT+PON vs. VCT+PON+BFA	2681	1469/1212	491	263/228
2. VCT+PON vs. VCT+PON+HYX	3609	1902/1707	355	187/168
3. genes commonly altered in 1 and 2	70	39/31	12	8/4

Figure 2. Global changes in gene expression with BFA and HYX stress. Expression profiles were obtained from VCT cells treated with 10 μM ponasterone A (PON) for 24 h in the presence or absence of 10 μg/ml brefeldin A (BFA) for 2 h, followed by a BFA-free recovery for 6 h (**1**.), or hypoxia (HYX) for 8 h (**2**.). The results shown are the number of genes and EST sequences altered in a given expression set comparison excluding those genes with variations in expression less than 2-fold (≥2-fold) or less than 5-fold (≥5-fold) between the two data sets compared. The number of genes/ESTs up- and down-regulated (+/-, respectively) for each comparison is shown. Also shown are data from the intersection of genes common to both the BFA and HYX stress responses (**3**.).

Figure 3. Global functional classifications of genes altered with brefeldin A (BFA) and/or hypoxic (HYX) stress. Genes with expression levels altered 2-fold and greater in the presence of BFA or HYX stress were analyzed by the DRAGON and HAPI databases to determine the major functional classification of the genes involved in the BFA (**A**, #1 comparison from Figure 2), HYX (**B**, #2 from Figure 2), and in both the BFA and HYX (**C**, #3 from Figure 2) stress responses. Shown are the percentage of genes from these comparisons whose primary functional classification was determined to be transcription regulation (trxn), cell cycle control (cell cycle), stress-responses (stress), tumor progression and growth (tumor growth), cell signaling (signaling), cell adhesion (adhesion), regulation of ion transport (ion reg.) regulation of calcium homeostasis (calcium homeo.) kinases or phosphatase activity (kinase/pptase), protein transport and shuttling (protein trans.) and protein modification and processing (protein mod.) apoptosis-related (apoptosis).

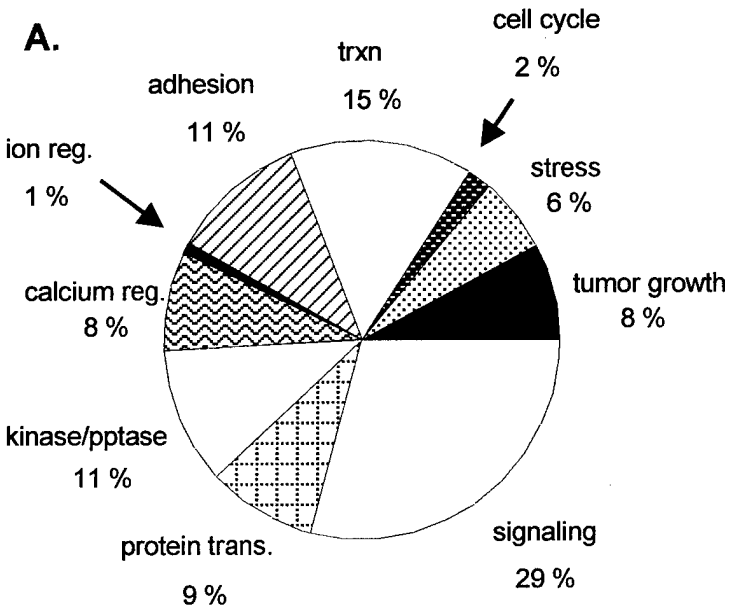

B.

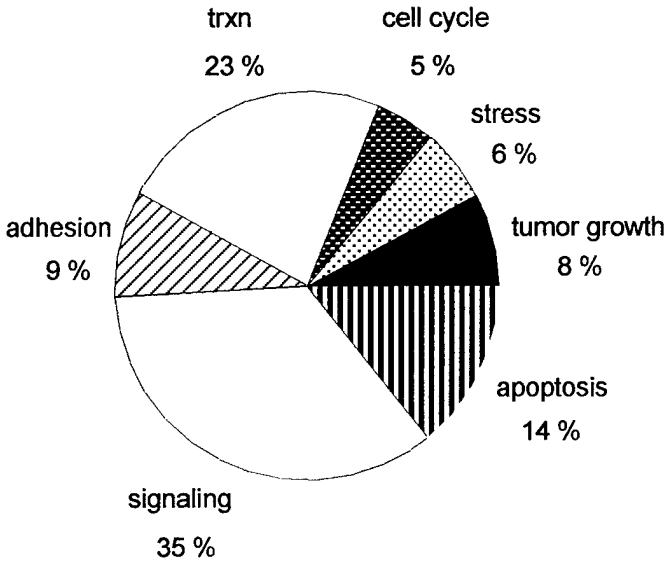
trxn
23 %
cell cycle
5 %
stress
6 %
tumor growth
8 %
apoptosis
14 %
signaling
35 %
adhesion
9 %

C.

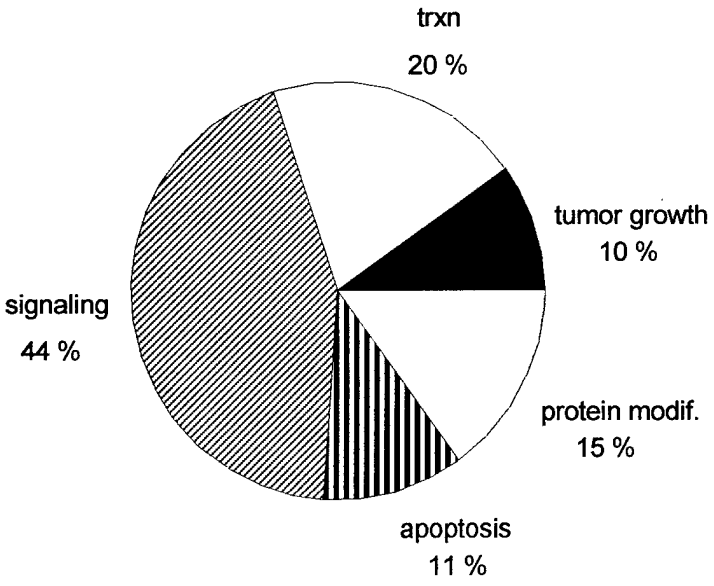
trxn
20 %
tumor growth
10 %
protein modif.
15 %
apoptosis
11 %
signaling
44 %

Figure 4. Genes commonly altered with either BFA or HYX stress treatment. Data shown are the relative fold changes in expression with BFA or HYX stress treatment for each gene altered at 2-fold and greater levels relative to unstressed control (#3 comparison from Figure 2). Also shown is the Affymetrix probe set identification number for each gene (probe set).

probe set	gene	BFA	HYX	
M27500_f_at	protamine	19.3	5.0	
AF015309_s_at	nucleolar protein (MSP58)	17.9	2.7	
M95200_s_at	vascular endothelial growth factor	17.2	19.2	
L13622_s_at	s-adenosylmethionine synthetase	16.2	11.4	
M64863_s_at	cytochrome P450 17-alpha hydroxylase C17/20 lyase	15.5	11.6	
AF000581_s_at	p300/CBP/Co-Integrator protein	8.4	2.3	
L28117_s_at	NF-kappaB (p105)	7.6	2.8	
J03962_s_at	acetylcholine receptor-associated protein (RAP-syn)	7.0	5.4	
Msa.1690.0_at	I-kappa B alpha	6.6	6.2	
M12572_at	heat shock protein (hsp68)	6.1	6.2	
L06443_s_at	putative transforming growth factor-beta	5.6	5.3	
U26188_s_at	B61	4.9	3.5	
L31783_s_at	uridine kinase	4.7	4.2	
L21221_s_at	proprotein convertase 4 (PC4)	4.4	2.0	
U77040_s_at	LIM protein 3 (mSLIM3)	4.3	2.8	
AB009287_s_at	macrosialin	3.4	2.7	
AF006688_at	peroxisomal acyl-CoA reductase (muspaox)	3.4	2.6	
D37793_s_at	synaptotagminII/IP4BP	3.4	2.9	
U92794_s_at	alpha glucosidase II beta subunit	3.4	2.1	
L04128_f_at	ribosomal protein L18 (rpL 18)	3.3	3.3	
L19737_f_at	H+ ATP synthase subunit c	3.1	4.0	
M37761_s_at	calcyclin	2.9	2.9	
M99054_s_at	acid phosphatase type 5	2.9	4.6	
D82019_s_at	basigin	2.8	2.8	
L14677_s_at	Epoc-1	2.8	2.0	
U73445_s_at	dihydrolipoamide dehydrogenase (Dld)	2.8	2.2	
U16162_s_at	prolyl 4-hydroxylase alpha (I)-subunit	2.7	3.4	up-regulated during BFA- and HYX-induced drug resistance
U59807_f_at	cystatin B (Stfb)	2.7	2.3	
D44443_s_at	dexamethasone-induced product	2.6	2.0	
AF022992_at	Rigui	2.5	3.5	
D13738_s_at	putative receptor tyrosine kinase	2.5	2.0	
U67188_s_at	G protein signaling regulator RGS5	2.5	2.0	
U28656_s_at	insulin-stimulated eIF-4E binding protein PHAS-I	2.4	2.5	
M55154_s_at	transflutaminase (TGase)	2.3	2.1	
U85489_s_at	Ah receptor-interacting protein (AIP)	2.3	2.6	
D13546_s_at	DNA polymerase alpha associated subunit	2.2	2.4	
L17076_s_at	RNA-binding protein	2.2	2.0	
U19520_s_at	vesicle transport protein munc-18b	2.1	2.8	
U30482_s_at	TR2	2.1	2.1	
D49956_s_at	8-oxo-dGTPase	-2.0	-2.2	
M32309_s_at	zinc finger protein Zfx	-2.0	-2.8	
D50494_s_at	murine RCK	-2.1	-2.6	
D37790_s_at	beta-1,4-galactosyltransferase	-2.2	-2.1	
U06922_s_at	signal transducer and activator of transcription Stat3	-2.2	-2.4	
U52524_s_at	hyaluronan synthase 2 (Has2)	-2.2	-2.5	down-regulated during BFA- and HYX-induced drug resistance
U85614_s_at	SRG3	-2.2	-2.4	
U63933_s_at	transcription factor IID (Tbp)	-2.3	-4.1	
U19891_s_at	putative CCAAT binding factor 1 (mCBF)	-2.4	-2.2	
M31810_s_at	2',3'-cyclic-nucleotide 3'-phosphodiesterase	-2.5	-2.9	
U92437_s_at	mutated in multiple cancers protein MMAC-1	-2.5	-2.1	
U70622_s_at	lysophosphatidic acid receptor (vzg-1)	-2.7	-2.4	
D38417_s_at	arylhydrocarbon receptor	-2.9	-3.3	
M22326-2_s_at	growth factor-induced protein zif/268	-2.9	-4.8	
U44088_s_at	TDAG51	-3.0	-4.3	
L29479_s_at	serine/threonine kinase (sak-a)	-3.1	-2.6	
M63650_s_at	M-twist	-3.2	-2.1	
U44725_s_at	mast cell growth factor Mgf	-3.3	-2.3	
U20238_s_at	GTPase-activating protein GAPIII	-3.6	-2.2	
U16322_s_at	basic transcription factor MITF-2B	-3.7	-3.2	
D78644_s_at	DNA polymerase	-3.9	-2.0	
U18869_s_at	mitogen-responsive phosphoprotein p96, alternatively spliced p67, and alternatively spliced p93	-4.2	-2.6	
D45210_f_at	zinc finger protein	-4.9	-2.1	
U27177_s_at	p107	-4.9	-2.7	
M69293_rc_at	Id-2	-5.2	-4.6	
L02526_s_at	protein kinase MEK	-5.4	-7.9	
M84607_s_at	platelet-derived growth factor-alpha receptor (PDGFRa)	-5.6	-5.3	
L35307_s_at	transcription regulator c-krox	-8.7	-3.7	
M64086_s_at	spi2 proteinase inhibitor (spi2-eb1)	-9.6	-7.8	
M93422_s_at	adenylyl cyclase type VI	-10.2	-9.8	

Figure 5. BFA and hypoxia treatment alter protein expression as suggested by expression profiling data. **A**. EMT6 cells were treated with either 10 μg/ml brefeldin A (BFA) for 2 h followed by a BFA-free recovery for 6 h, hypoxia (HYX) for 8 h, or 10 μg/ml castanospermine (CAS) for 6 h. Following treatment, whole cell lysates were collected and analyzed by western blot. The resulting membranes were probed with anti-TGFβ1 (TGF-β), anti-PDGFRα (PDGFRα), anti-MEK1 (MEK1), anti-MEK2 (MEK2), anti-phosphorylated-MEK1/2 (P-MEK1/2) and anti-actin (actin). Basal expression of each protein in the absence of stress is also shown (C). Shown is a representative blot from one of four independent experiments. **B**. Immunoblot band intensity was quantitated and expressed as the fold change in band intensity relative to non-treated control cells after correcting for variations in actin expression and background intensity. The data shown are the mean fold control change ± SEM in relative band intensity from four independent experiments. * - a statistically significant change in expression was observed with stress treatment when compared to non-treated control ($p<0.05$, ANOVA).

A.

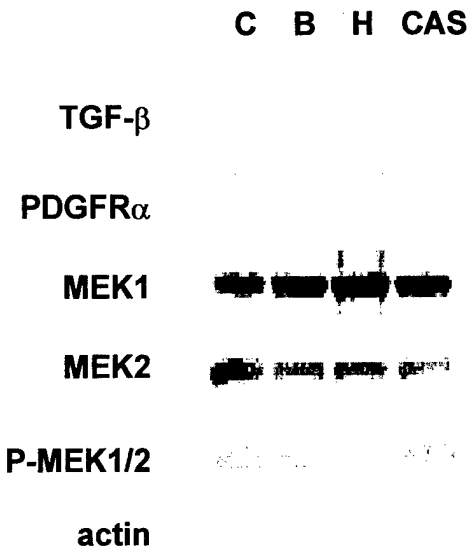
C B H CAS
TGF-β
PDGFRα
MEK1
MEK2
P-MEK1/2
actin

B.

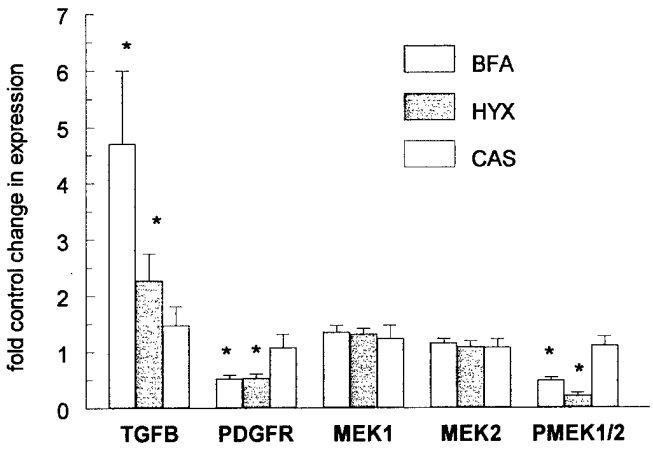
fold control change in expression
0
1
2
3
4
5
6
7
BFA
HYX
CAS
TGFB
PDGFR
MEK1
MEK2
PMEK1/2

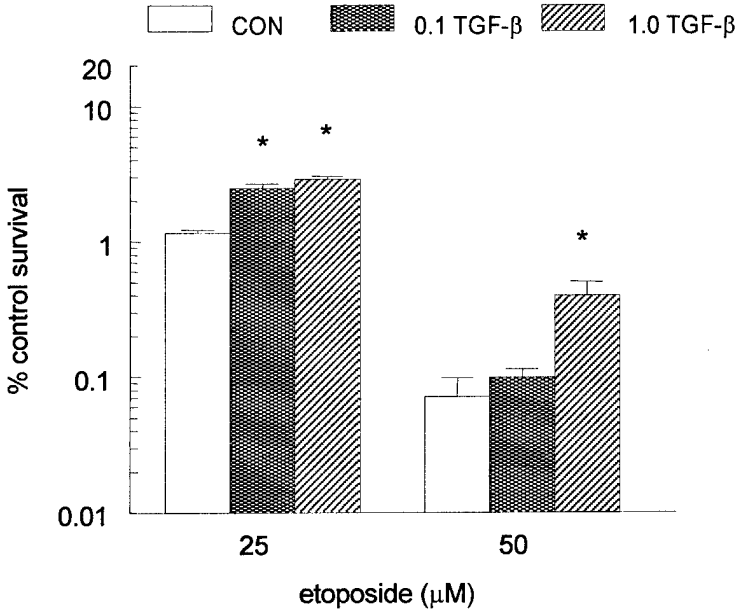

Figure 6. TGF-β treatment results in resistance to etoposide. EMT6 cells were treated with 0.1 or 1.0 ng/ml TGF-β (0.1 TGF-β and 1.0 TGF-β, respectively) for 8 h. During the last hour of treatment, 25 or 50 μM etoposide was added prior to analysis by colony forming assay. The toxicity of etoposide in non-stressed cells is also shown (CON). The results shown are the mean percent control changes in cell survival ± SEM from 4-6 independent experiments. * - a statistically significant increase in cell survival was observed with TGF-β treatment when compared to non-treated controls.

Figure 7. TGF-β treatment lowers PDGFRα and phosphorylated MEK protein levels. **A.** EMT6 cells were treated with 0.1 or 1.0 ng/ml TGF-β (0.1 TGF-β and 1.0 TGF-β, respectively) for 8 h. Following treatment, whole cell lysates were collected and analyzed by western blot. The resulting membranes were probed with anti-PDGFRα (PDGFRα), anti-MEK1 (MEK1), anti-MEK2 (MEK2), anti-phosphorylated-MEK1/2 (P-MEK1/2) and anti-actin (actin). Basal expression of each protein in the absence of stress is also shown (C). Shown is a representative blot from one of four independent experiments. **B.** Immunoblot band intensity was quantitated and expressed as a fold change in band intensity relative to non-treated control cells after correcting for variations in background intensity and actin expression. The data shown are the mean fold control change ± SEM in relative band intensity from four independent experiments. * - a statistically significant decrease in protein expression was observed in TGF-β-treated cells when compared to non-treated controls ($p<0.05$, ANOVA).

A.

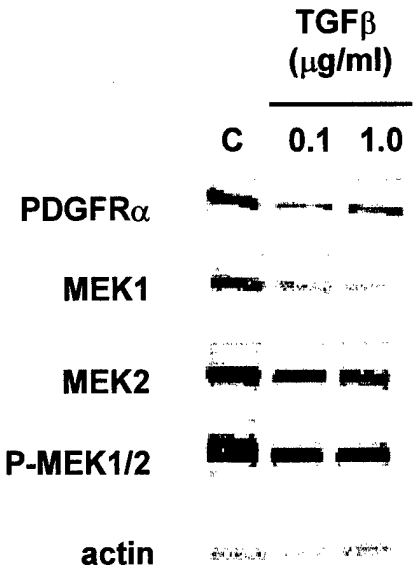
TGFβ
(μg/ml)
C
0.1
1.0
PDGFRα
MEK1
MEK2
P-MEK1/2
actin

B.

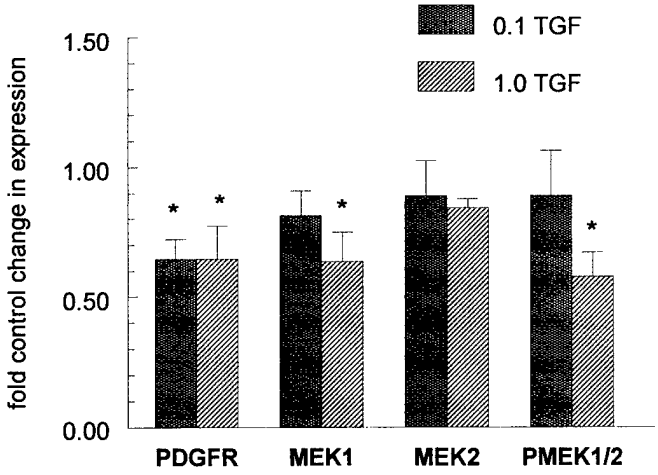
0.1 TGF
1.0 TGF
fold control change in expression
1.50
1.00
0.50
0.00
PDGFR
MEK1
MEK2
PMEK1/2

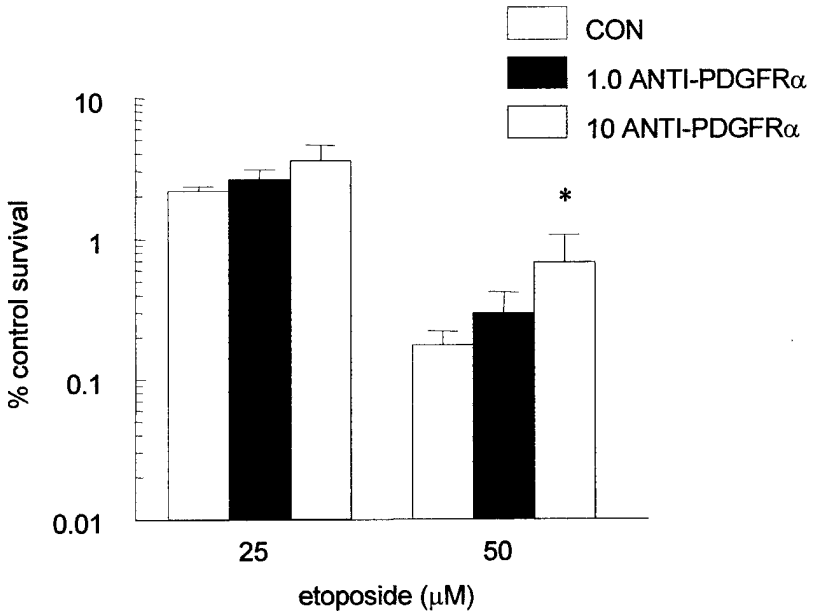

Figure 8. Treatment with an anti-PDGFRα blocking antibody induces resistance to etoposide. EMT6 cells were treated with 1.0 or 10 ng/ml anti-PDGFRα blocking antibody (1.0 anti-PDGFRα and 10 anti-PDGFRα, respectively) for 8 h. During the last hour of treatment, 25 or 50 μM etoposide was added prior to analysis by colony forming assay. The toxicity of etoposide in non-treated cells is also shown (CON). The results shown are the mean percent control cell survival ± SEM from 4-6 independent experiments. * - a statistically significant increase in cell survival was observed with anti-PDGFRα antibody treatment when compared to non-treated controls.

Figure 9. Treatment with an anti-PDGFRα blocking antibody (Ab) reduces phosphorylated MEK1/2 levels. **A.** EMT6 cells were treated with 1 or 10 ng/ml anti-PDGFRα blocking antibody (1.0 anti-PDGFRα and 10 anti-PDGFRα, respectively) for 8 h. Following treatment, whole cell lysates were collected and analyzed by western blot. The resulting membranes were probed with anti-MEK1 (MEK1), anti-MEK2 (MEK2), anti-phosphorylated-MEK1/2 (P-MEK1/2) and anti-actin (actin). Basal expression of each protein in the absence of stress is also shown (C). Shown is a representative blot from one of four independent experiments. **B.** Immunoblot band intensity was quantitated and expressed as a fold change in band intensity relative to non-treated control cells after correcting for variations in background intensity and actin expression. The data shown are the mean fold control change ± SEM in expression from four independent experiments. * - a statistically significant decrease in expression was observed with anti-PDGFRα antibody treatment when compared to non-treated controls ($p<0.05$, ANOVA).

A.

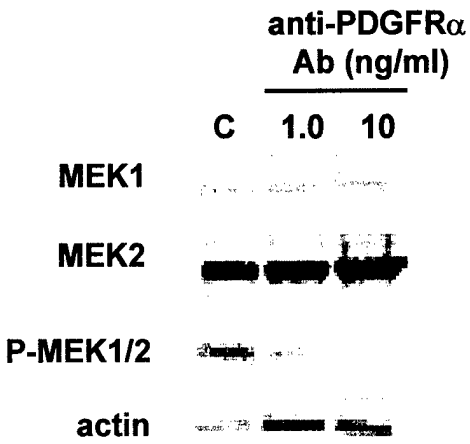
anti-PDGFRα
Ab (ng/ml)
C
1.0
10
MEK1
MEK2
P-MEK1/2
actin

B.

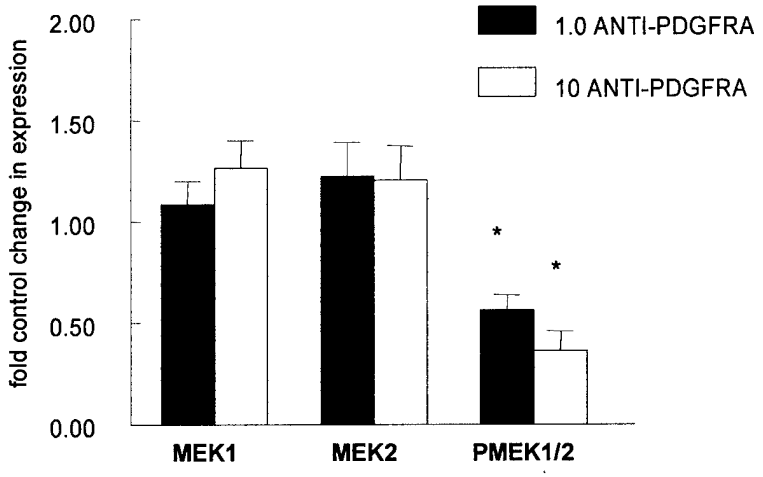
2.00
1.50
1.00
0.50
0.00
fold control change in expression
1.0 ANTI-PDGFRA
10 ANTI-PDGFRA
*
*
MEK1
MEK2
PMEK1/2

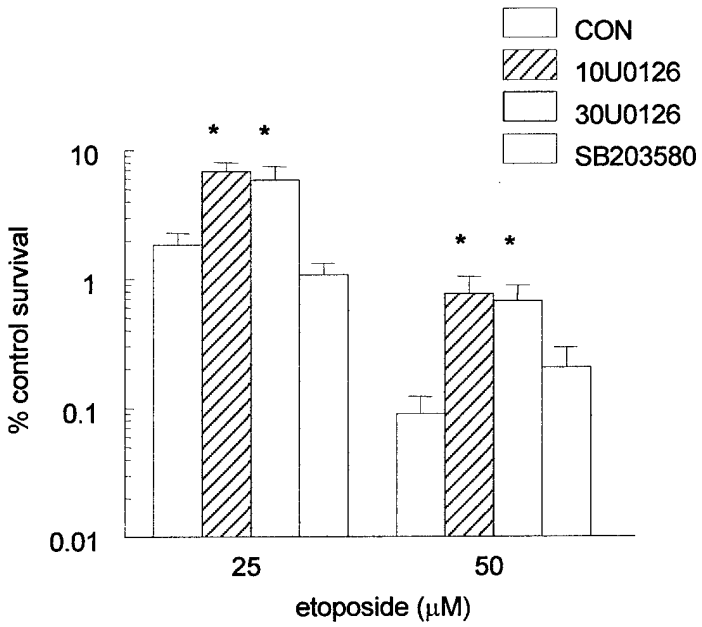

Figure 10. Treatment with the MEK1/2 inhibitor U0126, but not the p38 kinase inhibitor SB203580, induces resistance to etoposide. EMT6 cells were treated with 10 μM U0126 (10 U0126), 30 μM U0126 (30 U0126) or 10 μM SB203580 (SB203580) for 8 h. During the last hour of treatment, 25 or 50 μM etoposide was added prior to analysis by colony forming assay. The toxicity of etoposide on non-stressed cells is also shown (CON). The results shown are the mean percent control changes in cell survival ± SEM from 4-6 independent experiments. * - a statistically significant increase in cell survival was observed with U0126 treatment when compared to non-treated controls.

Figure 11. Treatment with U0126, but not SB203580, reduces phosphorylated MEK1/2 levels. **A.** EMT6 cells were treated with 10 μM U0126 (10 U0126), 30 μM U0126 (30 U0126) or 10 μM SB203580 for 8 h. Following treatment, whole cell lysates were collected and analyzed by western blot. The resulting membranes were probed with anti-MEK1 (MEK1), anti-MEK2 (MEK2), anti-phosphorylated-MEK1/2 (P-MEK1/2) and anti-actin (actin). Basal expression of each protein in the absence of stress is also shown (C). Shown is a representative blot from one of four independent experiments. **B.** Immunoblot band intensity was quantitated and expressed as a fold change in band intensity relative to non-treated control cells after correcting for variations in background intensity and actin expression. The data shown are the mean fold control change ± SEM in relative band intensity from four independent experiments. * - a statistically significant change in expression was observed in U0126-treated cells when compared to non-treated controls ($p<0.05$, ANOVA).

A.

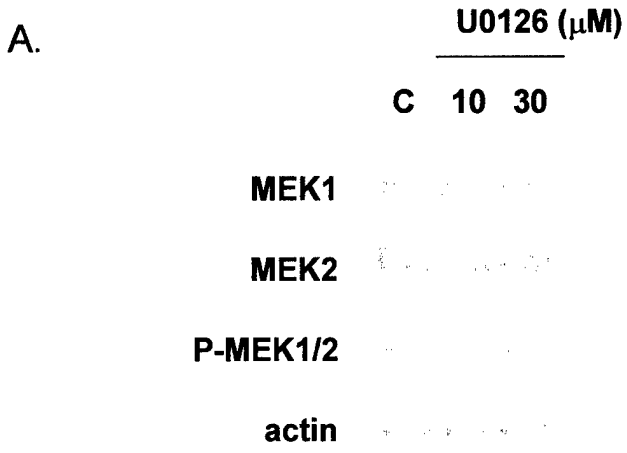
U0126 (μM)
C 10 30
MEK1
MEK2
P-MEK1/2
actin

B.

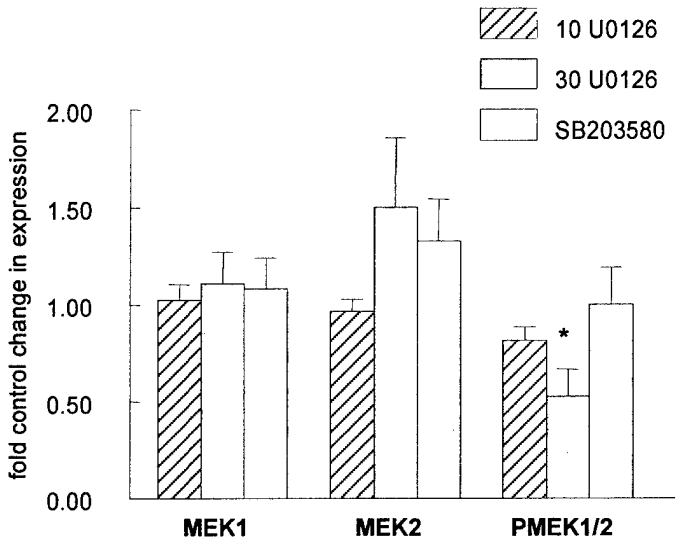
10 U0126
30 U0126
SB203580
fold control change in expression
2.00
1.50
1.00
0.50
0.00
*
MEK1
MEK2
PMEK1/2

Comparisons	≥2-fold	+/-	≥5-fold	+/-
4. VCT+PON+BFAvs.IκBαM+PON+BFA	3478	2149/1329	42	25/17
5. VCT+PON+HYXvs.IκBαM+PON+HYX	1447	873/574	18	8/10
6. genes commonly altered in 4 and 5	40	22/18	0	0/0

Figure 12. Global changes in gene expression during the reversal of BFA- and HYX-induced resistance with IκBαM. Expression profiles were obtained from VCT and IκBαM cells treated with 10 μM ponasterone A (PON) for 24 h in the presence or absence of 10 μg/ml brefeldin A (BFA) for 2 h, followed by a BFA-free recovery for 6 h (**4**.), or hypoxia (HYX) for 8 h (**5**.). The results shown are the number of genes and EST sequences altered in a given expression set comparison excluding those genes with variations in expression less than 2-fold (≥2-fold) or less than 5-fold (≥5-fold) between the two data sets compared. The number of genes/ESTs up- and down-regulated (+/-, respectively) for each comparison is shown. Also shown are data from the intersection of genes involved in the reversal of both BFA- and HYX-induced resistance with IκBαM (**6**.).

Figure 13. Global functional classifications of genes altered in the reversal of BFA- and HYX-induced resistance with IκBαM. Genes with expression levels altered 2-fold and greater in the reversal of BFA- and HYX-induced resistance with IκBαM were analyzed by the HAPI and DRAGON expression databases to determine the major functional classification of the genes involved in the reversal of either BFA- (**A**, #4 comparison from Figure 12), HYX- (**B**, #5 from Figure 12), or both BFA- and HYX-induced drug resistance (**C**, #6 from Figure 12). Shown are the percentage of genes from these comparisons whose primary functional classification was determined to be transcription regulation (trxn), cell cycle control (cell cycle), oncogenesis (oncogenes), tumor progression and growth (tumor growth), cell signaling (signaling), cell adhesion (adhesion), and protein modification and processing (protein mod.), apoptosis-related (apoptosis), glycosylation (glycosylation), DNA binding proteins (DNA binding), cholesterol biosynthesis (cholest. synth.), protease activity (protease) and development (development).

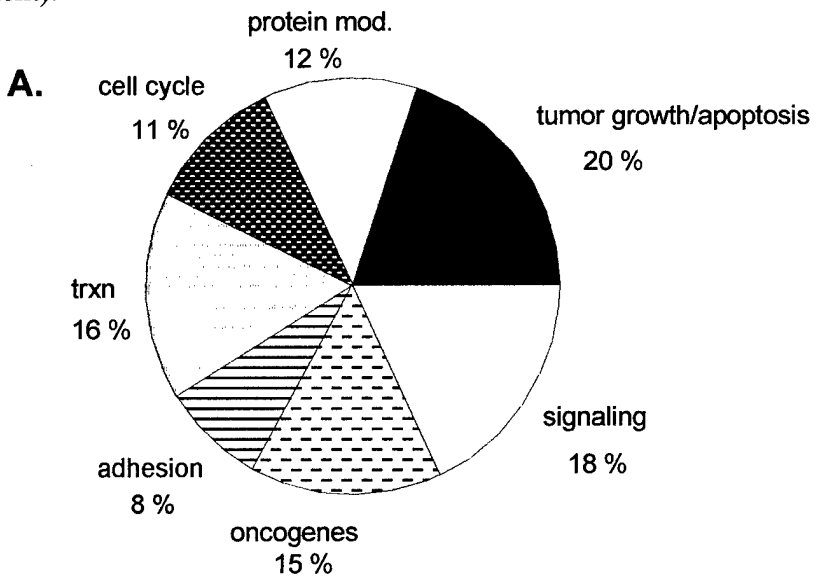

B.

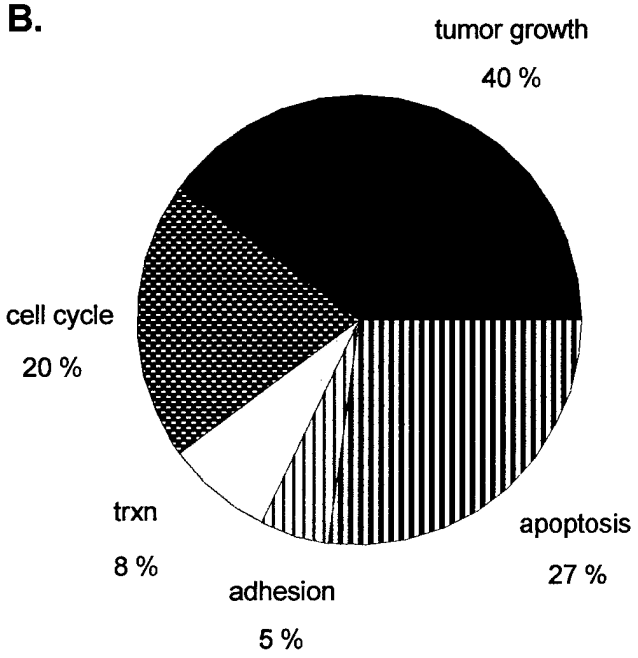
tumor growth
40 %
cell cycle
20 %
trxn
8 %
adhesion
5 %
apoptosis
27 %

C.

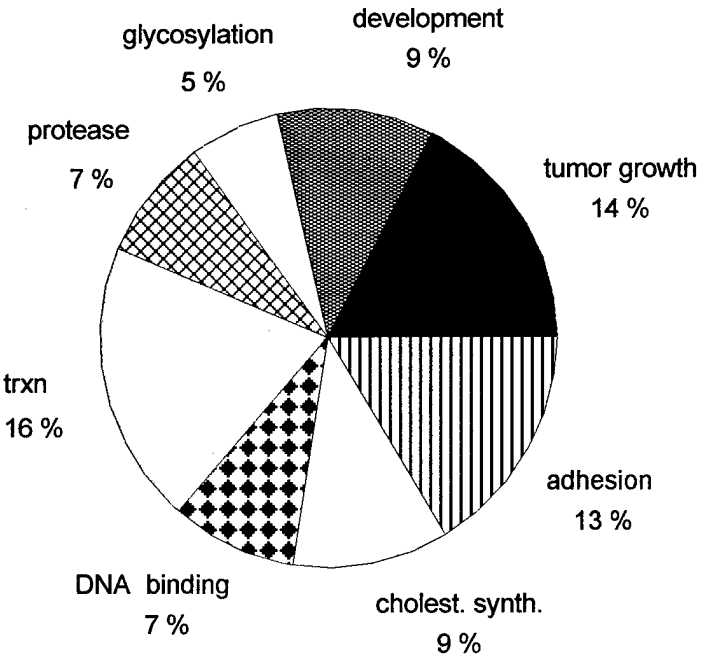
glycosylation
5 %
development
9 %
protease
7 %
tumor growth
14 %
trxn
16 %
adhesion
13 %
DNA binding
7 %
cholest. synth.
9 %

Figure 14. Genes altered during the reversal of BFA-induced drug resistance with IκBαM expression. Data shown are the mean fold changes in expression for each gene altered 5-fold and greater when comparing expression profiles of induced IκBαM cells treated with BFA to induced VCT cells treated with BFA (#4 comparison from Figure 12). Also shown is the Affymetrix probe set identification number for each gene.

downregulated in IκBαM cells			upregulated in IκBαM cells		
probe set	geneID	mean	probe set	geneID	mean
M19380	Calmodulin (camIII)	-15.2	Msa.1581.0	Cytokeratin 15	6.9
X63099	Connexin31	-9.7	Msa.2646.0	Crkl	6.9
AF026537	Prodynorphin	-9.6	Msa.574.0	Cytochrome c	6.9
I31532	bcl-2	-8.7	Msa.2710.0	Syndecan	7
J05154	Cholest. Acyltransferse LCAT	-8.5	Z21848	DNA polymerase delta	9.1
D28132	PACAP/VIP receptor 3	-8.1	u08439	Cytochrome c oxidase ViaH	9.3
ET62336	DNA ligase III beta	-8.1	Msa.2694.0	Sp1	9.6
M93422	Adenylyl cyclase type VI	-7.9	u10530	SNO protooncogene prot. DE3	9.7
Msa.4.0	Apolipoprotein E	-7.7	Msa.1078.0	cAMP-dep. prot. kinase type II	9.8
Msa.2217.0	c-myb oncogene	-7.6			
U37017	Vav2 oncogene	-7.4			
L32752	GTPase (ran)	-7.3			
X64534	IL-3	-7.1			
d89571	Ryudocan core protein	-6.4			
u18867	Uroporphyrinogen III synthase	-6.4			
L35032	HMG-box trxn factor sox18	-6.3			
Msa.1586.0	TIS11	-6.2			
Msa.669.0	GABAa	-6.2			
X67083	Chop-10	-6			
af031956	Tcl1 oncogene	-6			
Msa.628.0	FgfK	-5.8			
Msa.540.0	Connexin30.3	-5.6			
L35302	TRAF1 TNF-assoc. fact. 1	-5.4			
d55720	Nuc. Pore targeting complex	-5.4			
Msa.2435.0	MAPK-activ. prot kinase 2	-5.4			
AB00678	Apoptosis signal-reg kinase	-5.3			
D83674	MesP1	-5.3			
u96724	Phosphoinositide-5-P'ase II	-5.2			
x15373-2	P400	-5.2			
j03723	Carbohydrate binding prot. 35	-5.1			
X92498	fkh-6	-5.1			
m83749	D type cyclin (CYL2)	-5.1			
M13806	Keratin type 1	-5			

downregulated in IκBαM cells

probe set	geneID	mean
m92649	nitric oxide synthase	-81.6
m28698	Cytokeratin 19	-70.5
x61940	GF-inducible immediate gene 3CH134	-12
m22115	ERA-1-993	-11.6
msa.788.0	HLH DNA binding protein Id	-10.6
u78031	bcl-X	-7.2
x61232	Carboxypeptidase H	-5.7
m33960	Plasminogen activator inhibitor (PAI-1)	-5.6
x83601	PTX3	-5.3
u52073	TDD5	-5.1
m64292	TIS21	-5

upregulated in IκBαM cells

probe set	geneID	mean
L28177	GADD45	5
u20735	jun B	5
et61021	N23K devel. regulated molecule	5
msa.3205.0	ADP-ribosylation factor-like protein 4	5
u14729	Addressin cell adhesion mol.(madcam1)	5
x59421	fli-1	5

Figure 15. Genes altered during the reversal of HYX-induced drug resistance with IκBαM expression. Data shown are the mean fold changes in expression for each gene altered 5-fold and greater when comparing expression profiles of induced IκBαM cells treated with HYX to induced VCT cells treated with HYX (#5 comparison from Figure 12). Also shown is the Affymetrix probe set identification number for each gene.

Figure 16. Genes commonly altered during the reversal of both BFA- and HYX-induced drug resistance with IκBαM expression. Data shown are the intersection of mean fold changes in expression for each gene altered 2-fold and greater when comparing expression profiles of induced IκBαM cells treated with BFA to induced VCT cells treated with BFA and IκBαM cells treated with HYX to induced VCT cells treated with HYX (#6 comparison from Figure 38). Also shown is the GenBank identification number for each gene.

GenBank #	Gene ID	BFA	HYX	
msa.907.0	4-1BB ligand	15.4	4.8	
y12783	ring1B	7.2	2.6	
x17617	ZFP-35	6.3	4.7	
x80903	delta-like protein 1	6.3	3.1	
v00727	c-fos	5.2	2.6	
x55499	Ig/EBP-1	4.4	5.4	
x71327	MRE-binding trxn factor	4.2	7	
msa.2251.0	D3 dopamine receptor	3.9	2.1	
x06746	Krox-20	3.3	2.3	
x58472	kif-17	3.2	2.4	
z19581	siah-2	2.7	2.5	
et61251	serine/threonine kinase FNK	2.4	4.6	
msa.2694.0	Sp1	2.4	4.6	
z31278	T-ZAP	2.4	2.3	up-regulated during the reversal of both BFA- & HYX-induced drug resistance with IκBαM
msa.2759.0	voltage dependent Na+ chan. Beta1 sub.	2.3	2.9	
X64414	low density lipoprotein receptor	2.3	2.3	
msa.3143.0	tumor associated glycoprotein E4	2.2	3.6	
x68804	MMCP-4 protease	2.2	4.2	
y00864	c-kit	2.2	2	
msa.756.0	HMG CoA reductase	2.1	3.7	
x16995	N10 nuclear hormone binding receptor	2	2.2	
msa.43191.0	integrin-associated protein	-2	-5	
x56603	calcium binding protein	-2	-2.8	
msa.226.0	cytochrome c oxidase	-2.1	-3.5	down-regulated during the reversal of both BFA- & HYX-induced drug resistance with IκBαM
msa.1690.0	IkappaBalpha	-2.6	-2	
y07711	zyxin	-2.6	-2	
L23423	alpha 7 integrin	-2.7	-2.7	
msa.2967.0	ANP clearance receptor	-2.7	-2.3	
v00835	metallothionein I	-2.8	-2.6	
x86405	CB2 cannabinoid receptor	-3.2	-2.2	
y07941	plakophilin I	-3.2	2	
et62444	sox4	-3.5	-2.9	
AF006492	friend of GATA-1	-5.9	-2.7	
U77083	CD13 aminopeptidase N	-6	-2.2	
AF007267	sec53p	-7.3	-2.9	
msa.464.0	bcl-3	-7.4	-3.4	
D45889	PG-M core protein	-8.2	-3	
I35307	c-Krox	-8.2	-2.8	
x53798	MIP2	-20.1	-3.9	
x67083	chop10	-30.6	-4.4	

Figure 17. Expression of IκBαM prevents stress-induced enhancement of TGF-β expression. Vector-transfected cells (VCT) and IκBαM-expressing cells (IκBαM) were treated with 10 μM ponasterone A (PON) for 24 h to induce gene expression. Cells were treated in the presence of PON with either 10 μg/ml brefeldin A (B) for 2 h followed by a BFA-free recovery for 6 h or with hypoxia (H) for 8 h. **A.** Whole cell lysates were collected and analyzed by western blot. The resulting membranes were probed with anti-TGF-β (TGF-β) or anti-actin (actin) primary antibodies. The level of protein expression in the absence of stress (C) is also shown for each cell type. Shown is one representative blot from three independent experiments. **B.** The relative band intensity from three independent experiments was quantitated using the Scion Image program (www.scioncorp.com), converted into a ratio of protein band intensity to background intensity, and then adjusted based upon the ratio of protein band intensity to background intensity for the housekeeping gene actin. Corrected intensities were then reported as a fold-control change ± SEM in expression with stress treatment.

A.

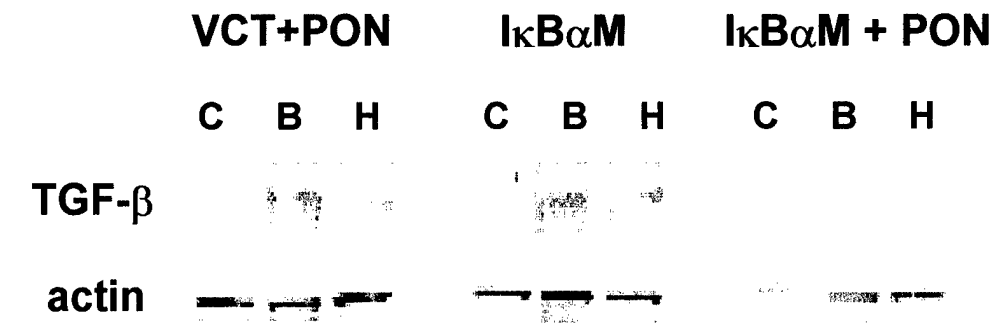
VCT+PON
IκBαM
IκBαM + PON
C B H C B H C B H
TGF-β
actin

B.

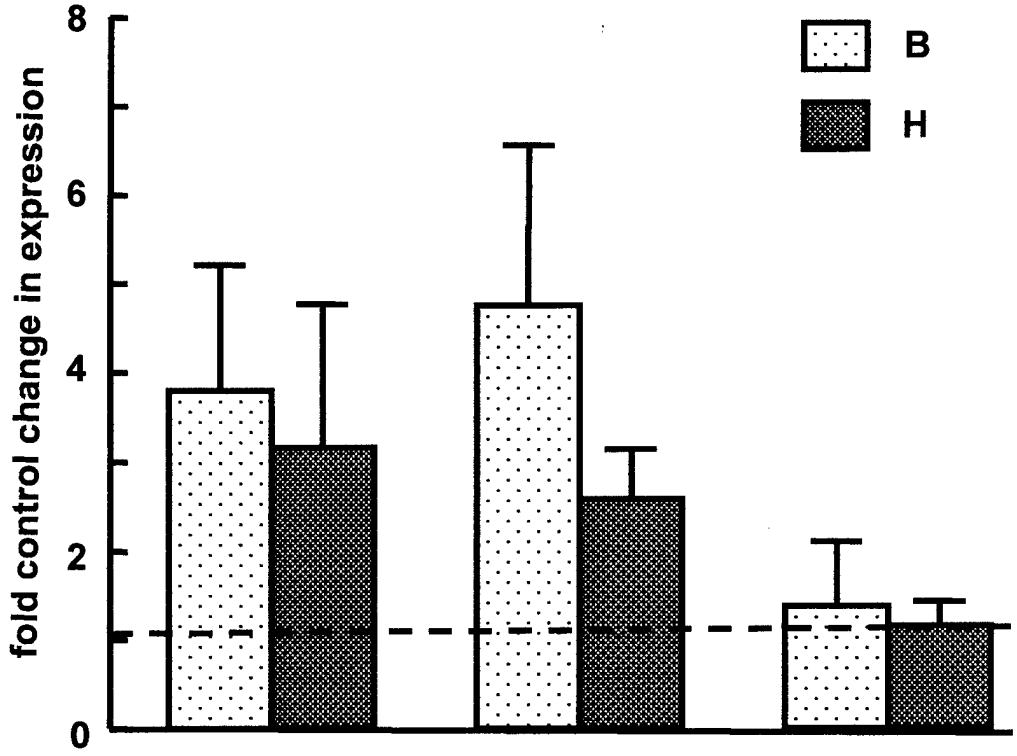
fold control change in expression
0
2
4
6
8
B
H

Figure 18. Expression of IκBαM prevents stress-induced inhibition of PDGFRα expression. Vector-transfected cells (VCT) and IκBαM-expressing cells (IκBαM) were treated with 10 μM ponasterone A (PON) for 24 h to induce gene expression. Cells were treated in the presence of PON with either 10 μg/ml brefeldin A (B) for 2 h followed by a BFA-free recovery for 6 h or with hypoxia (H) for 8 h. **1.** Whole cell lysates were collected and analyzed by western blot. The resulting membranes were probed with anti-PDGFRα (PDGFRα) primary antibody. The level of protein expression in the absence of stress (C) is also shown for each cell type. Shown is one representative blot from three independent experiments. **2.** The relative band intensity from three independent experiments was quantitated using the Scion Image program (www.scioncorp.com), converted into a ratio of protein band intensity to background intensity, and then adjusted based upon the ratio of protein band intensity to background intensity for the housekeeping gene actin (shown in Figure 17). Corrected intensities were then reported as a fold-control change ± SEM in expression with stress treatment. *, a statistically significant decrease in PDGFRα expression was observed with stress treatment ($p<0.05$, ANOVA).

A.

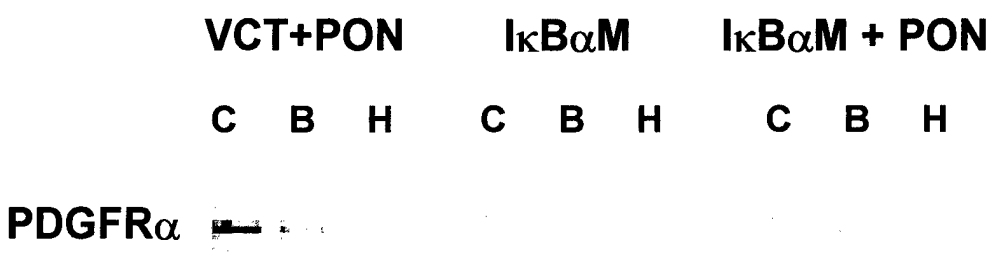
VCT+PON
IκBαM
IκBαM + PON
C B H C B H C B H
PDGFRα

B.

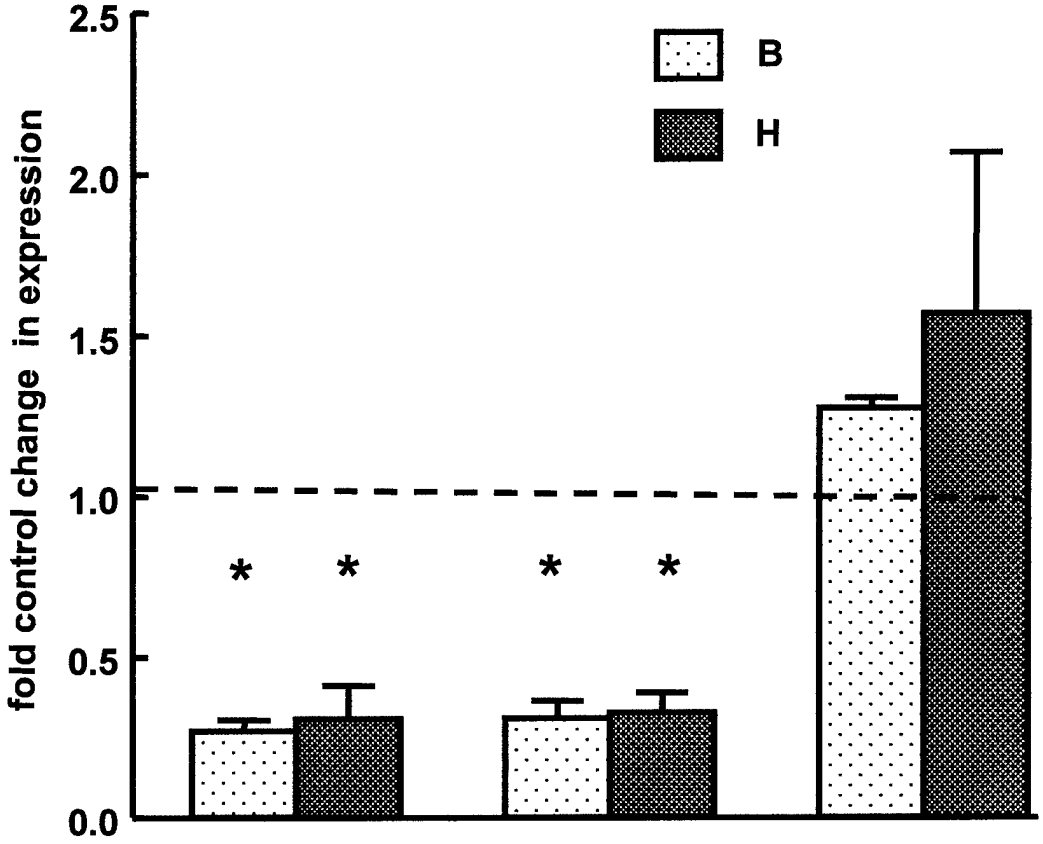
2.5
2.0
1.5
1.0
0.5
0.0
fold control change in expression
B
H
*
*
*
*

Figure 19. Expression of IκBαM prevents stress-induced inhibition of MEK1/2 phosphorylation. Vector-transfected cells (VCT) and IκBαM-expressing cells (IκBαM) were treated with 10 μM ponasterone A (PON) for 24 h to induce gene expression. Cells were treated in the presence of PON with either 10 μg/ml brefeldin A (B) for 2 h followed by a BFA-free recovery for 6 h or with hypoxia (H) for 8 h. **1.** Whole cell lysates were collected and analyzed by western blot. The resulting membranes were probed with anti-MEK1 (MEK1), anti-MEK2 (MEK2) and anti-phosphorylated-MEK1/-MEK2 (P-MEK1/2) primary antibodies. The level of protein expression in the absence of stress (C) is also shown for each cell type. Shown is one representative blot from three independent experiments. **2.** Quantitation of P-MEK1/2 protein levels. The relative band intensity from three independent experiments was quantitated using the Scion Image program (www.scioncorp.com), converted into a ratio of protein band intensity to background intensity, and then adjusted based upon the ratio of protein band intensity to background intensity for the housekeeping gene actin (shown in Figure 17). Corrected intensities were then reported as a fold-control change ± SEM in expression with stress treatment. *, a statistically significant decrease in P-MEK1/2 expression was observed with stress treatment ($p<0.05$, ANOVA).

A.

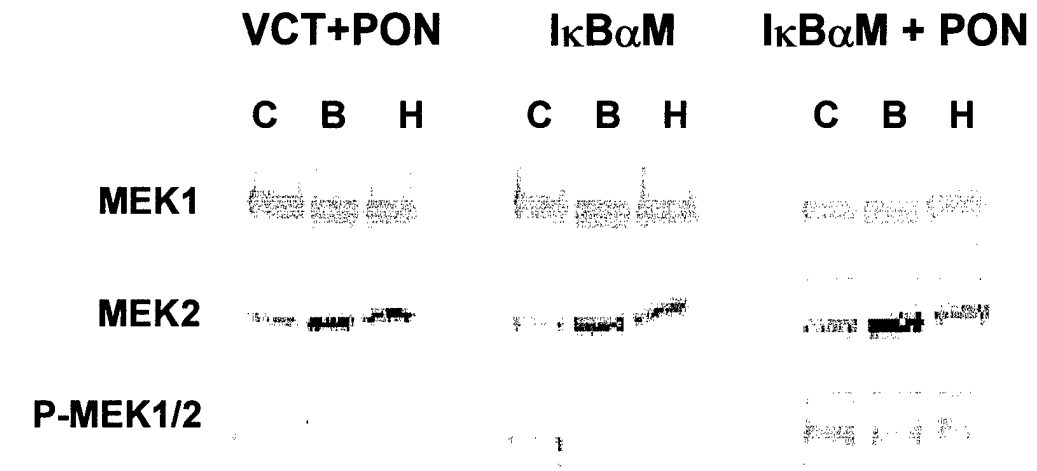
VCT+PON
IκBαM
IκBαM + PON
C B H
C B H
C B H
MEK1
MEK2
P-MEK1/2

B.

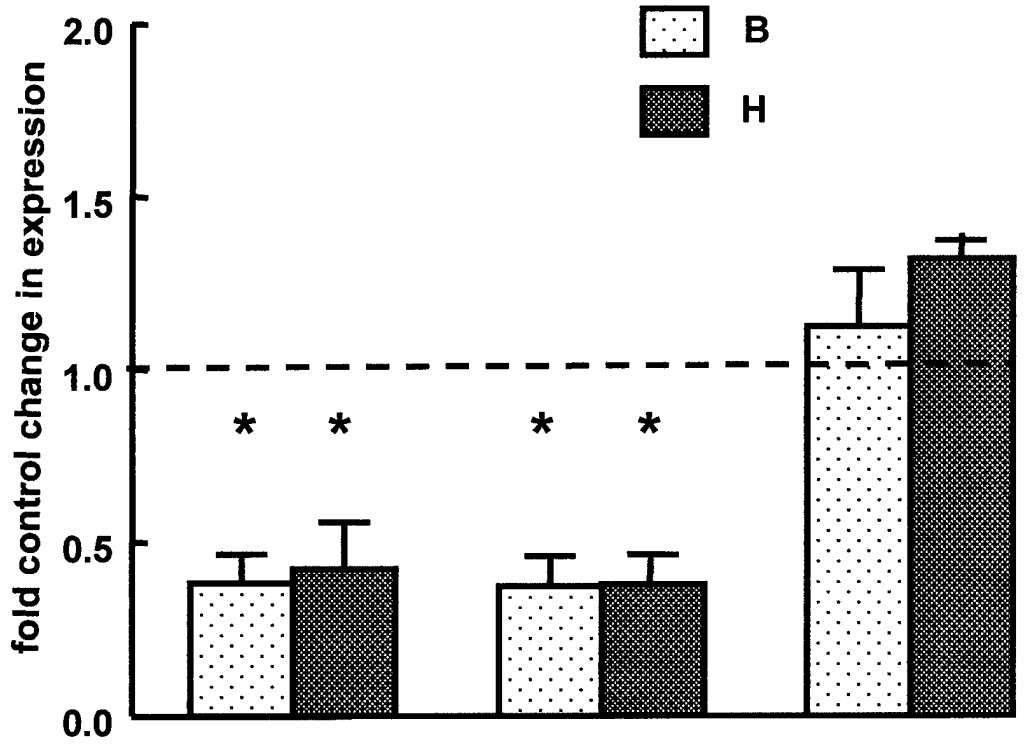
B
H
fold control change in expression
2.0
1.5
1.0
0.5
0.0
*
*
*
*